Vibrational Analysis of Nucleic Acids. 2. Ab Initio Calculation of the Molecular Force Field and Normal Modes of Dimethyl Phosphate†

Yifu Guan, Godwin S.-C. Choy,‡ Rainer Glaser,‡ and George J. Thomas, Jr.*

Division of Cell Biology and Biophysics, School of Biological Sciences, University of Missouri—Kansas City, Kansas City, Missouri 64110

Received: March 2, 1995; In Final Form: May 25, 1995⊗

The *gauche−gauche* (*g,g*) conformation of the dimethyl phosphate anion serves as a simple model for the phosphodiester group of nucleic acids. Detailed knowledge of the normal modes of vibration of dimethyl phosphate and other phosphodiester analogues is expected to provide a foundation for understanding the conformation-sensitive bands in vibrational spectra of DNA and RNA. In the previous paper of this series (Guan, Y.; et al. *Biophys. J.* **1994**, *66*, 225−235), infrared and Raman spectra of the *g,g* conformer of dimethyl phosphate [$(CH_3O)_2PO_2^-$], including deuterium [$(CD_3O)_2PO_2^-$] and carbon-13 [$(^{13}CH_3O)_2PO_2^-$] isotopomers, were reported and assigned in conjunction with a complete normal coordinate analysis. The normal mode calculations were accomplished by use of a generalized valence force field. Here, we demonstrate that an ab initio molecular force field for the *g,g* conformer of dimethyl phosphate, computed using the 3-21+G* basis set, is consistent with the empirically based valence force field reported previously. We have obtained the force field scaling factors which produce satisfactory agreement between the calculated and experimental vibrational frequencies of each of the three dimethyl phosphate isotopomers in the *g,g* conformation. Ab initio normal mode assignments, in terms of the potential energy distribution, are in general accord with those obtained from the normal coordinate analysis. Agreement between the ab initio and normal coordinate results supports the reliability of the empirically derived force field for extension to other phosphodiester conformations of dimethyl phosphate, as well as to more complex diester derivatives of the nucleic acid orthophosphate group.

Introduction

Vibrational spectroscopy is a sensitive and versatile probe of nucleic acid structures and interactions. The usefulness of the method depends upon the accuracy of vibrational assignments and the reliability of correlations between macromolecular conformation and spectral parameters. (Specific applications are considered in recent review articles.[1,2]) An important consideration in applications to DNA or RNA is the reliability of vibrational assignments for the normal modes of the sugar−phosphate backbone. This is of particular significance in the case of Raman spectroscopy. For example, although several intense Raman bands can be identified with phosphodiester linkages of DNA[3] and RNA,[4] the internal coordinates which define the normal modes of vibration are not yet known in detail for a single Raman band of the nucleic acid backbone. The application of Raman spectroscopy in structural studies of nucleic acids would benefit greatly from knowledge a priori of the relationships between backbone conformation and both the *frequencies* and *intensities* of vibrational bands. Recently, we have initiated work in this area through normal coordinate analysis of the nucleic acid phosphodiester group[5] and by computation of the Raman tensors of oriented DNA molecules in crystals and fibers.[6,7]

To develop an understanding of the normal coordinates associated with vibrational modes of the nucleic acid backbone, we are conducting experimental and theoretical studies of isotopically labeled nucleic acid analogues. In the previous paper of this series,[5] we reported infrared and Raman spectra of several dimethyl phosphate (DMP) isotopomers, including the normal DMP molecule [$(CH_3O)_2PO_2^-$, DMP-h_6], the deuteriomethyl derivative [$(CD_3O)_2PO_2^-$, DMP-d_6] and the carbon-13 derivative [$(^{13}CH_3O)_2PO_2^-$, DMP-$^{13}C_2$]. Dimethyl phosphate serves as the simplest structural analogue of the phosphodiester network (C−O−P−O−C) in DNA or RNA. The experimental data obtained on DMP isotopomers have been employed to construct a generalized valence force field (GVFF) which satisfactorily reproduces all of the experimentally observed Raman and infrared frequencies.[5] In the present paper, we report the results of ab initio calculation of the DMP force field, and compare the results with the empirically based valence force field developed previously. The present calculations employ the 3-21+G* basis set[8] for determination of the vibrational frequencies. We also compare results of the 3-21+G* calculations with those obtained using smaller (3-21G*) and larger (6-311+G*) basis sets for the DMP anion.

The ab initio approach requires the molecular geometry as input and provides as output a comprehensive molecular force field, including diagonal and off-diagonal elements of the force constant matrix upon which the normal modes depend.[9] In previous ab initio studies of DMP, the smaller 3-21G basis set was employed and elements of the force constant matrix were not determined.[10,11] Scaling factors, which are required to bring ab initio and experimental vibrational frequencies into accord with one another, also were not reported in the previous studies.

The specific objectives of the present work are threefold. First, we seek to obtain ab initio vibrational spectra (infrared and Raman frequencies and intensities) of DMP for comparison with experimental data, thereby determining an optimal set of scaling factors for future applications to other nucleic acid analogues. Second, we propose to evaluate the ab initio and empirically determined molecular force fields for consistency

† Supported by NIH Grant AI18758.
‡ Permanent address: Department of Chemistry, University of Missouri, Columbia, MO 65211.
* To whom correspondence may be addressed.
⊗ Abstract published in *Advance ACS Abstracts*, July 1, 1995.

0022-3654/95/2099-12054$09.00/0

with one another and to establish guidelines in the selection of off-diagonal force constants that can be used in future valence force field calculations. Finally, we employ the present results as a test of key Raman and infrared band assignments, proposed previously on the basis of experimentally observed isotopic shifts in the spectral frequencies.[5]

Methods

1. Computations. Ab initio calculations using the Gaussian 90 program[8] were performed on a Model 3090 mainframe computer (IBM Corp., Armonk, NY) accessed with an Iris personal computer (Silicon Graphics, Mountain View, CA). Coordinate transformations were performed with the GZINT[12] program operating on a VAX Station 3100 (DEC, Nashua, NH) as described previously.[5]

The structure of each DMP anion (DMP-h_6, DMP-d_6, and DMP-$^{13}C_2$) was optimized in the *gauche*−*gauche* (*g,g*) conformation at the restricted Hartree−Fock level. Harmonic vibrational frequencies and the molecular force field in terms of Cartesian coordinates were calculated using Gaussian 90. The optimized structure was used to develop a set of 36 internal coordinates and to construct the **B** matrix, allowing conversion from Cartesian to internal coordinates. The **U** matrix, which permits analysis of the harmonic vibrational frequencies in terms of the potential energy distribution (PED) among symmetry coordinates, was calculated using GZINT[12] and additional computational routines provided by Prof. C. J. Wurrey, Department of Chemistry, University of Missouri, Kansas City. The latter programs also permitted calculation of infrared and Raman intensities as well as force constants in terms of either Cartesian or internal coordinates for comparison with the previously reported results of normal coordinate analysis.[5]

2. Experimental Data. Experimental vibrational frequencies are those reported in FTIR and Raman spectra of solids and solutions of DMP-h_6, DMP-d_6, and DMP-$^{13}C_2$.[5]

Results and Discussion

1. Ab Initio Optimization of the Dimethyl Phosphate Structure. We seek to optimize the conformation of the phosphodiester skeleton (C−O−P−O−C) of DMP, as a model for the 5′C−O−P−O−3′C network in a nucleic acid backbone. In RNA, as well as in the *A* form of DNA, X-ray structures of oligonucleotide single crystals[13] show that the *gauche* conformation is preferred nearly exclusively for both the 5′O−P and 3′O−P torsions (α and ζ, respectively; see Figures 1 and 2). This nucleic acid backbone geometry is usually designated by the notation g^-,g^-. The g^-,g^- conformation is also preferred, though less exclusively, for α and ζ torsions in the *B* form of DNA. (The available X-ray data indicate a small but significant number of nucleotide residues with ζ in the *trans* domain, i.e., g^-,t conformation.) The experimentally determined α and ζ torsions of *A*-form and *B*-form oligonucleotide crystal structures exhibit the distributions shown in the histograms of Figure 2. Accordingly, for DMP, we proceed with ab initio optimization of the *g,g* conformation.

Experimental evidence that the *g,g* conformation of the aqueous DMP anion is favored energetically over other rotamers is provided by vibrational spectroscopy,[5,14,15] and the experimental results are supported by a large body of theoretical evidence.[11,16−20] Additionally, the X-ray crystal structure of the ammonium salt of dimethyl phosphate[21] indicates the *g,g* conformation as the only rotamer in the crystal. With the availability of the NH_4DMP crystal structure, it is also appropriate to consider ab initio optimization of the NH_4^+:$(CH_3O)_2PO_2^-$ ion pair.

TABLE 1: Structure Parameters Obtained by ab Initio Optimization and X-ray Crystallography

	ab initio calculations				
	DMP anion			NH_4DMP	crystal data
structure parameter[a]	3-21G*	3-21+G*	6-311+G*	3-21G*	(NH_4DMP)[b]
		Bond Length			
P-O	1.473	1.489	1.468	1.498	1.490, 1.498
P−O	1.634	1.635	1.633	1.587	1.536, 1.582
C−O	1.435	1.445	1.393	1.454	1.425, 1.481
C-H[c]	1.083	1.082	1.086	1.079	
		Valence Angle			
∠O-P-O	124.58	124.16	124.60	113.72	117.2
∠O−P−O	98.27	99.62	99.94	103.92	104.8
∠P−O−C	118.21	121.86	120.20	121.64	123.0, 118.3
∠O−C-H[c]	109.24	108.94	110.13	108.80	
∠H-C-H[c]	109.31	108.94	108.81	110.13	
		Torsion			
(O−P−O−C)	74.90	77.20	75.90	77.39	57.5, 62.4

[a] Bond lengths are in angstroms; valence angles and torsions are in degrees. [b] From ref 21. [c] Average of symmetry related parameters.

a. Comparison between the DMP Anion and the NH_4DMP Ion Pair. Structures of the NH_4DMP ion pair and isolated DMP anion were fully optimized in C_2 symmetry using the 3-21G* basis set.[8] This basis set is composed of the doubly split valence orbitals with polarization functions on the phosphorus atom. Table 1 summarizes the geometric parameters of both optimized structures. For comparison, the experimentally determined structure parameters of NH_4DMP[21] are included in Table 1. It should be noted that, in the crystal structure, DMP does not exhibit rigorous C_2 symmetry, evidenced by small differences in the ester bond lengths and angles (last column of Table 1).

Table 1 shows that the 3-21G* optimized structure (column 5) of the phosphate group in the NH_4DMP ion pair is in excellent agreement with the crystal structure (column 6). The calculated phosphodioxy P-O bond length (1.498 Å) is essentially identical to the crystallographic values (1.498, 1.490 Å), and the calculated phosphodiester P−O bond length (1.587 Å) is only marginally larger (1.536, 1.582 Å). Similarly, good agreement exists between calculated and experimental values of the C−O bond length and all valence angles. Although hydrogen atoms are not located in the X-ray structure, their optimized parameters (average values) are in agreement with standard experimental values for similar model compounds. Table 1 thus indicates that the 3-21G* basis set is sufficient for satisfactory optimization of the NH_4DMP structure. The only significant discrepancy in the optimized structure occurs for O−P−O−C torsion angles (≈77°), which are close to 60° in the crystal structure, a probable consequence of crystal packing.

Table 1 also lists optimized parameters for the isolated DMP anion. Comparison with NH_4DMP (column 5) indicates that the NH_4^+ cation exerts a significant structural effect on DMP. The optimized P-O and C−O bonds of DMP are shorter than those of NH_4DMP by 0.025 and 0.019 Å, respectively, while the P−O bonds are longer by 0.047 Å. Corresponding differences are observed in valence and torsion angles. These effects can be rationalized as the result of electrostatic attraction between NH_4^+ and DMP^-, which causes reductions in the O-P-O valence angle and P−O bond length and increases in the O−P−O valence angle and P-O bond length.[13,22,23] On the other hand, the O−P−O−C torsion angle is only marginally affected by lattice pairing with NH_4^+.

b. Basis Set Dependence of the Calculations. Three different basis sets, 3-21G*, 3-21+G*, and 6-311+G*, were employed for the DMP structure optimization. The results are given in columns 2−4, respectively, of Table 1. (In comparison

TABLE 2: Symmetry Coordinates of Dimethyl Phosphate Anion

symmetry coordinate (unnormalized)	description[a]
A Species	
$S1 = r1 + r2$	$\nu_s(PO_2^-)$
$S2 = r3 + r4$	$\nu_s(PO_2)$
$S3 = r5 + r9$	$\nu_s(CO)$
$S4 = r6 + r7 + r8 + r10 + r11 + r12$	$\nu_s(CH_3)$
$S5 = 2r6 - r7 - r8 + 2r10 - r11 - r12$	$\nu_a(CH_3)$
$S6 = \alpha13$	$\delta(PO_2^-)$
$S7 = \alpha18$	$\delta(OPO)$
$S8 = \alpha19 + \alpha20$	$\delta_s(POC)$
$S9 = 2\alpha21 - \alpha22 - \alpha23 + 2\alpha27 - \alpha28 - \alpha29$	$r(CH_3)$
$S10 = \alpha21 + \alpha22 + \alpha23 - \alpha24 - \alpha25 - \alpha26 + \alpha27 + \alpha28 + \alpha29 - \alpha30 - \alpha31 - \alpha32$	$\delta_s(CH_3)$
$S11 = -\alpha24 - \alpha25 + 2\alpha26 - \alpha30 - \alpha31 + 2\alpha32$	$\delta_a(CH_3)$
$S12 = \tau33 + \tau34$	$\tau_s(O-P-O-C)$
$S13 = \tau35 + \tau36$	$\tau_s(P-O-C-H)$
$S14 = r7 - r8 + r11 - r12$	$\nu_a(CH_3)$
$S15 = \alpha14 - \alpha15 - \alpha16 + \alpha17$	$\tau(PO_2^-)$
$S16 = \alpha22 - \alpha23 + \alpha28 - \alpha29$	$r(CH_3)$
$S17 = \alpha24 - \alpha25 + \alpha30 - \alpha31$	$\delta_a(CH_3)$
B Species	
$S18 = r1 - r2$	$\nu_a(PO_2^-)$
$S19 = r3 - r4$	$\nu_a(PO_2)$
$S20 = r5 - r9$	$\nu_a(CO)$
$S21 = r6 + r7 + r8 - r10 - r11 - r12$	$\nu_s(CH_3)$
$S22 = 2r6 - r7 - r8 - 2r10 + r11 + r12$	$\nu_a(CH_3)$
$S23 = \alpha14 - \alpha15 + \alpha16 - \alpha17$	$\omega(PO_2^-)$
$S24 = \alpha19 - \alpha20$	$\delta_a(POC)$
$S25 = \alpha22 - \alpha23 - \alpha28 + \alpha29$	$r(CH_3)$
$S26 = \alpha24 - \alpha25 - \alpha30 + \alpha31$	$\delta_a(CH_3)$
$S27 = r7 - r8 - r11 + r12$	$\nu_a(CH_3)$
$S28 = \alpha14 + \alpha15 - \alpha16 - \alpha17$	$r(PO_2^-)$
$S29 = 2\alpha21 - \alpha22 - \alpha23 - 2\alpha27 + \alpha28 + \alpha29$	$r(CH_3)$
$S30 = \alpha21 + \alpha22 + \alpha23 - \alpha24 - \alpha25 - \alpha26 - \alpha27 - \alpha28 - \alpha29 + \alpha30 + \alpha31 + \alpha32$	$\delta_s(CH_3)$
$S31 = -\alpha24 - \alpha25 + 2\alpha26 + \alpha30 + \alpha31 - 2\alpha32$	$\delta_a(CH_3)$
$S32 = \tau33 - \tau34$	$\tau_a(O-P-O-C)$
$S33 = \tau35 - \tau36$	$\tau_a(P-O-C-H)$

[a] Abbreviations: ν stretching, δ bending, ω wagging, r rocking, t twisting, τ torsion, s symmetric, a antisymmetric.

to the 3-21G* set, 3-21+G* includes additional diffuse functions on C, O, and P atoms, while 6-311+G* contains triply split valence orbitals together with polarization and diffuse functions.[8,24]) The 3-21+G* set yields somewhat better agreement with the NH_4DMP crystal structure than does 3-21G*, particularly for P-O bond lengths, while the 6-311+G* set yields no obvious advantages over the smaller basis sets. We conclude that for these compounds structure optimization is not significantly improved by use of the 6-311+G* basis set, and we have therefore employed the 3-21+G* basis set in subsequent force field calculations. The fact that the smaller basis set reduces computational time without significant loss of accuracy is relevant to our long range goal of applying ab initio calculations to other phosphodiester analogs of DNA.

2. Ab Initio Vibrational Frequencies and Force Field for DMP-h_6. *a. Overview.* Calculated (3-21+G*) vibrational frequencies were classified by use of the **U** matrix into *A* and *B* symmetry blocks, in accordance with the global C_2 symmetry of the DMP anion. The 33 nonredundant symmetry coordinates are listed in Table 2, and the corresponding 36 internal coordinates are shown in Figure 1. Vibrational assignments were made on the basis of the potential energy distributions (PED), in terms of symmetry coordinates. The **U** matrix was constructed making use of both the global C_2 symmetry of the DMP anion and the local C_{3v} symmetry of each methyl group. Table 3, which summarizes the results for DMP-h_6, lists the

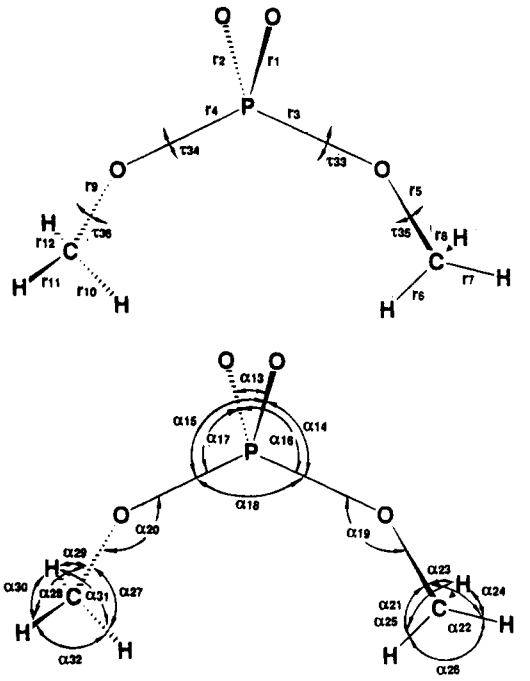

Figure 1. Internal coordinates of the *gg* conformer of dimethyl phosphate anion. Top: Stretching and torsion coordinates. (Note that torsion coordinates $\tau33$ and $\tau34$ correspond to nucleic acid phosphodiester torsions α and ζ. See discussions in text.) Bottom: Bending coordinates.

unscaled ab initio vibrational frequencies (column 1), the scaled ab initio vibrational frequencies (column 2), the ab initio PED values (column 3), the observed Raman frequencies (column 4), the PED values based upon normal coordinate analysis[5] (column 5), and the proposed assignment for each vibrational mode (column 6). The unscaled ab initio frequencies of Table 3 are, as expected, generally 10−15% higher than the observed frequencies. However, a few notable exceptions are apparent, and these are discussed in the subsequent sections.

The unscaled frequencies have been corrected using a standard scaling procedure.[9,26,27] With the appropriate choice of internal-coordinate-dependent scaling factors (footnote a, Table 3), the average error between calculated and experimental frequencies has been reduced to 9.86 cm^{-1} (0.87%).

The scaled ab initio vibrational frequencies and Raman and infrared intensities can be used to simulate Raman and infrared spectra of DMP-h_6 (Figure 3). The top plot in each panel of Figure 3 shows the calculated spectrum, in which the position and length of each vertical bar represent, respectively, the frequency and relative intensity of the vibrational band. The bottom plot in each panel is the observed spectrum recorded at the experimental conditions indicated. The calculated Raman and infrared spectra demonstrate good agreement with the experimental spectra.

b. Phosphate Group Vibrations. The calculated P−O (phosphoester single bond) symmetric and antisymmetric stretching frequencies are 777 and 818 cm^{-1}. Although these unscaled values are 3% higher and 1% lower, respectively, than the experimental frequencies of 754 and 827 cm^{-1}, it is interesting to note that Liang et al.[11] reported similar exceptionally low frequencies in their 6-31G* ab initio calculations on DMP-h_6. Table 3 shows as well that the unscaled ab initio frequency for the symmetric P-O (phosphodioxy) stretching mode is lower (1162 cm^{-1}) than the frequency of the C−O symmetric stretching mode (1173 cm^{-1}), an observation also reported by Hadzi[10] and Liang.[11] (Ordinarily, the partial double bond character of the phosphodioxy linkages should elevate its

TABLE 3: Vibrational Frequencies and Potential Energy Distributions for DMP-h_6[a]

ab initio (cm^{-1})					
unscaled	scaled	ab initio PED (%)	Raman (cm^{-1})	NCA PED (%)	assignment
			A Species		
3279	3024	S5(59), S14(41)	3021	S5(100)	$\nu_a(CH_3)$
3253	3000	S14(52), S5(40)	2997	S14(100)	$\nu_a(CH_3)$
3192	2943	S4(92)	2915	S4(100)	$\nu_s(CH_3)$
1668	1486	S11(90)	1464	S11(82)	$\delta_a(CH_3)$
1652	1472	S17(92)	1464	S17(82)	$\delta_a(CH_3)$
1604	1450	S10(96)	1450	S10(100)	$\delta_s(CH_3)$
1291	1187	S9(78)	1192	S9(69), S11(18)	$r(CH_3)$
1265	1158	S16(94)	1159	S16(70), S17(18), S12(12)	$r(CH_3)$
1162	1085	S1(49), S3(20), S2(19)	1083	S1(91)	$\nu_s(PO_2^-)$
1173	1060	S3(48), S1(42)	1058	S3(37), S10(27), S2(17)	$\nu_s(CO)$
777	749	S2(58), S3(28)	754	S2(30), S3(16), S9(16), S6(16)	$\nu_s(PO_2)$
550	513	S6(44), S7(36)	504	S6(27), S8(26), S7(26)	$\delta(PO_2^-)$
411	389	S15(51), S7(20), S8(13)	393	S15(29), S13(29), S12(26)	$\tau(PO_2^-)$
387	362	S6(46), S7(26), S15(12), S8(11)	367	S6(30), S7(24), S13(24)	$\delta(OPO)$
231	216	S8(64), S15(28)	(205)	S13(50), S8(44)	$\delta_s(POC)$
124	124	S13(92)	(142)	S13(90)	$\tau_s(P-O-C-H)$
83	83	S12(89), S7(10)	(72)	S12(94)	$\tau_s(O-P-O-C)$
			B Species		
3279	3023	S22(60), S27(39)	3021	S22(99)	$\nu_a(CH_3)$
3252	3000	S27(54), S22(39)	2997	S27(99)	$\nu_a(CH_3)$
3191	2942	S21(92)	2915	S21(96)	$\nu_s(CH_3)$
1667	1484	S31(91)	1464	S31(82)	$\delta_a(CH_3)$
1653	1472	S26(89)	1464	S26(82)	$\delta_a(CH_3)$
1606	1451	S30(93)	1450	S30(89)	$\delta_s(CH_3)$
1370	1264	S18(95)	1217	S18(41), S28(27), S29(32)	$r(CH_3)$
1288	1182	S29(84)	1192	S29(65), S31(17)	$r(CH_3)$
1266	1158	S25(94)	1158	S25(64), S26(16)	$\nu_a(PO_2^-)$
1153	1047	S20(72), S19(21)	1037	S20(35), S17(13), S28(13)	$\nu_a(CO)$
818	795	S19(61), S20(21), S23(16)	827	S19(25), S23(25), S20(14)	$\nu_a(PO_2)$
592	559	S28(45), S23(31), S24(17)	539	S28(24), S23(21), S32(21)	$r(PO_2^-)$
492	466	S23(52), S28(23)	476	S23(49), S28(48)	$\omega(PO_2^-)$
225	211	S24(67), S28(24)	(233)	S24(58), S33(45)	$\delta_a(POC)$
144	143	S33(68), S32(23)	(166)	S33(71), S32(29)	$\tau_a(P-O-C-H)$
105	105	S32(71), S33(28)	(108)	S32(53), S33(47)	$\tau_a(O-P-O-C)$

av error = 9.86 cm^{-1} (0.87%)

[a] Ab initio calculations employ the 3-21+G* basis set with the following scaling factors: 0.85 for P-O stretching, 1.0 for P−O stretching, 0.79 for O−C stretching, 0.85 for C-H stretching, 0.85 for O-P-O bending, 0.9 for O−P-O bending, 0.86 for O−P−O bending, 0.85 for P−O−C bending, 0.84 for O−C-H bending and 0.79 for H-C-H bending and 1.0 for torsions. Only potential energy distributions larger than 10% are listed and symmetry coordinates are defined in Table 2. Raman frequencies and NCA PED values are from ref 5. Other notation is defined in Table 2 or the text.

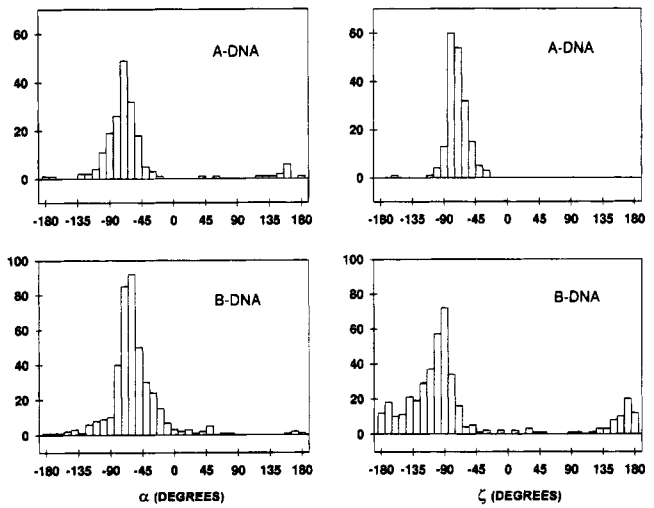

Figure 2. Histograms showing relative distributions of torsion angles α (left) and ζ (right) in crystal structures of A-DNA (top) and B-DNA (bottom). Data were obtained from 50 oligonucleotide crystal structures deposited in the Brookhaven Databank and Nucleic Acid Database.

symmetric stretching frequency to a value significantly higher than the symmetric C−O stretching frequency.[1-5,14]) The unusually low phosphate group frequencies can be reckoned with other ab initio frequencies of DMP by the standard procedure of selecting internal-coordinate-dependent scaling factors (footnote *a*, Table 3).[26,27]

After scaling, small discrepancies persist only in a few *B* species modes. Specifically, the antisymmetric phosphodioxy and phosphodiester stretching modes are, respectively, 47 cm^{-1} (4%) higher and 32 cm^{-1} (4%) lower than the experimental frequencies. The first of these discrepancies, reported also by both Hadzi[10] and Liang,[11] can be explained as a phosphate group hydration effect, i.e., the experimental frequency in DMP (1217 cm^{-1}) is lowered vis-à-vis the ab initio frequency as a consequence of interactions of DMP with solvent H_2O molecules. This is consistent with the shift of the 1240 cm^{-1} band of crystalline DMP to 1217 cm^{-1} in aqueous solution[5] and with similar results reported in other investigations. For example, infrared and Raman spectra demonstrate that hydration of DNA lowers the antisymmetric phosphate mode from 1240 to 1220 cm^{-1}, while very little change is observed in the corresponding symmetric mode.[28-30] Similar hydration effects have been reported for phosphate group modes of phospholipid head groups[31,32] and related phosphoesters.[33,34]

We note that the present interpretation is supported by normal coordinate calculations which show that changes in phosphodiester torsion angles (τ33 and τ34, Figure 1) are not alone sufficient to generate the substantial changes in phosphodioxy group frequencies which accompany hydration.[30,35] Hydration

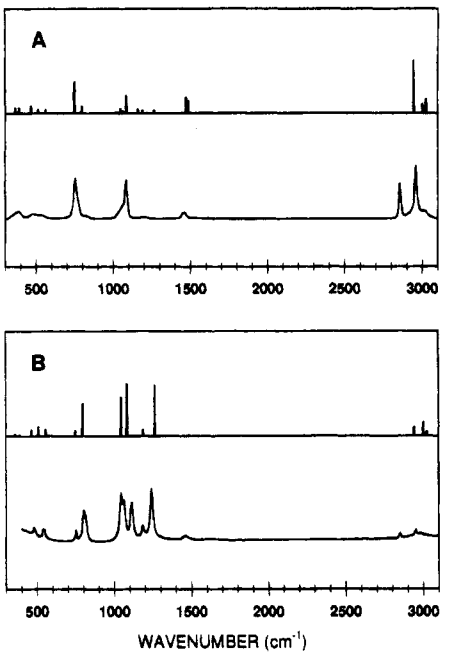

Figure 3. Raman (A) and infrared (B) vibrational spectra of DMP-h_6. In each panel the calculated ab initio frequencies and calculated intensities are represented as bars (upper plots) and the experimental spectrum[5] is shown as smooth curve (lower plot).

may also be invoked to account for the discrepancy in calculated and experimental values of the antisymmetric phosphodiester stretching mode. We note, for example, that the Raman frequency in the DMP crystal (802 cm^{-1}) is lower than that observed for the solution state (827 cm^{-1}).[5] Similar results are observed for DNA.[28,30]

The scaled ab initio frequencies which correspond to phosphate group bending modes, viz., rocking, wagging and twisting of the PO_2^- group, match the observed frequencies fairly well. Additionally, the PED values (Table 3) indicate that PO_2^- bending modes do not couple significantly with vibrations of the DMP skeleton or methyl groups. This suggests that the respective low-frequency bands in spectra of DNA and RNA may be useful as indicators of interaction between the backbone phosphodioxy groups and biologically important ligands.

c. Carbon–Oxygen Stretching Frequencies. Table 3 shows that the ab initio frequency of the symmetric C–O stretching mode (1060 cm^{-1}) is higher than that of the antisymmetric mode (1047 cm^{-1}), which is consistent with our previous normal coordinate calculations based upon experimental data from DMP isotopomers.[5] In previous vibrational studies of nucleic acids[1,2,6,7] and model compounds,[14,15,25] efforts to assign C–O stretching frequencies have yielded mixed results. In some cases,[14,15] the frequencies within the 1000–1100 cm^{-1} interval have been unassigned; in others, the assignments[25] have been contradicted by later work.[11] The assignments of Table 3 are based upon comprehensive experimental data from infrared, Raman, depolarization and isotopic shift measurements and are supported by both empirical (NCA) and ab initio force field calculations.

The ab initio PED values of Table 3 indicate that symmetric P-O stretching (symmetry coordinate S1) as well as symmetric C–O stretching (S3) are involved in the 1060 cm^{-1} normal mode. On the other hand, normal coordinate analysis predicts coupling of symmetric P–O stretching (S2) and symmetric methyl deformation (S10) with S3. This discrepancy can be rationalized as a consequence of the different force fields used in NCA and ab initio calculations, specifically, a result of the inequivalent off-diagonal force constants. The DMP force field will be discussed in greater detail in sections **2.e** and **2.f.** below.

d. Methyl Group Frequencies. The scaled ab initio frequencies for methyl stretching and bending modes are, with one exception, in good agreement with the experimental frequencies and normal coordinate calculations. One strong Raman band is predicted for symmetric C-H stretching, while two bands of nearly equal Raman intensity are observed (top panel, Figure 3). The observed doublet can be attributed to Fermi resonance involving the symmetric C-H stretching fundamental and the first overtone of the methyl deformation mode.[5,39] The Fermi resonance is not taken into account in the ab initio calculations.

Slight discrepancies between ab initio and NCA PED values can also be recognized in Table 3, columns 3 and 5. These are attributed to deviations of DMP methyl groups from strict C_{3v} symmetry, which is assumed in NCA calculation of the **U** and **G** matrices but not in ab initio optimization of the DMP structure.

e. Diagonal Force Constants. By use of the **B** matrix and scaling factors, the ab initio molecular force field in terms of Cartesian coordinates was converted to the force field in terms of internal coordinates. The resulting 36 diagonal and 630 off-diagonal elements can be compared with the generalized valence force field of Guan et al.[5] Such a comparison for bond stretching force constants is given in Table 4. (A comprehensive tabulation of diagonal and off-diagonal force constants corresponding to all internal coordinates of Figure 1, including valence angles and torsions, is available as supplementary material or from the authors upon request.)

The ab initio force constant of 8.527 mdyn $Å^{-1}$ for P-O stretching (internal coordinates $r1$ and $r2$, Table 4) is within 0.2% of the GVFF value of 8.541 mdyn $Å^{-1}$. Similarly, for C–O ($r5$, $r9$) and C-H stretching ($r6$, $r7$, $r8$; $r10$, $r11$, $r12$), the ab initio force constants of Table 4 are in very close agreement with the indicated GVFF values. The small differences among calculated C-H stretching constants reflect the slight deviation of the optimized methyl group structure from C_{3v} symmetry. For P–O stretching ($r3$, $r4$), the calculated force constant of 5.353 mdyn $Å^{-1}$ is 8% higher than the GVFF value of 4.928 mdyn $Å^{-1}$.[5] Collectively, the ab initio force constants for stretching modes of DMP are in excellent agreement with the GVFF results.[5] Accordingly, the bond stretching force constants of the empirical force field can be transferred reliably for normal-coordinate analyses of other DMP conformers.

Ab initio diagonal force constants for the DMP bending modes, designated as $\alpha 13$–$\alpha 32$ (Figure 1), are also in reasonably good agreement with corresponding GVFF values. These are indicated in the footnote of Table 4. We note that the ab initio bending constants take into account explicitly the slightly asymmetric phosphate group of the optimized structure. Thus, for example, two distinct O-P–O bending force constants (1.208 and 1.292 mdyn Å rad^{-2}) contribute to an average value (1.250 mdyn Å rad^{-2}) which compares favorably with the GVFF result[5] (1.446 mdyn Å rad^{-2}). A significant discrepancy for O-P-O bending (a13), i.e., 0.887 vs 1.510 mdyn Å rad^{-2}, presumably represents the effect of hydration of the DMP anion, as noted by others.[10,29] For torsional modes, the ab initio and GVFF force constants exhibit the type of semiquantitative agreement observed in related applications.[9,38]

f. Off-Diagonal Force Constants. Off-diagonal force constants represent interactions between two stretching or bending modes sharing a common atom or bond. For example, the off-diagonal force constant located at the crossing point of row $r1$ and column $r2$ of Table 4 represents interaction between

TABLE 4: Ab Initio and GVFF Force Constants for Stretching Coordinates of DMP[a]

	*r*1	*r*2	*r*3	*r*4	*r*5	*r*6	*r*7	*r*8	*r*9	*r*10	*r*11	*r*12
*r*1	8.527 (8.541)	0.195 (0.725)	0.284 (0.673)	0.321 (0.673)	−0.052	0.011	0.023	0.007	−0.110	0.016	0.006	0.029
*r*2		8.527 (8.541)	0.321 (0.673)	0.284 (0.673)	−0.110	0.016	0.006	0.029	−0.052	0.011	0.023	0.007
*r*3			5.353 (4.928)	0.400 (0.316)	0.123 (0.094)	−0.052	−0.036	−0.073	−0.077	0.028	0.014	0.005
*r*4				5.354(4.928)	−0.077	0.028	0.014	0.005	0.123 (0.094)	−0.052	−0.036	−0.073
*r*5					4.635 (4.693)	0.187 (0.555)	0.150 (0.555)	0.149 (0.555)	0.020 (0.108)	−0.002	−0.006	−0.003
*r*6						4.858 (4.953)	0.066 (0.005)	0.061 (0.005)	−0.002	0.001	0.001	0.000
*r*7							4.955 (4.953)	0.057(0.005)	−0.006	0.001	0.001	0.001
*r*8								4.990 (4.953)	−0.003	0.000	0.001	0.001
*r*9									4.635 (4.693)	0.187 (0.555)	0.150(0.555)	0.149 (0.555)
*r*10										4.858 (4.953)	0.066 (0.005)	0.061 (0.005)
*r*11											4.956 (4.953)	0.057(0.005)
*r*12												4.990 (4.953)

[a] Units are mdyn Å^{-1}. GVFF values[5] are in parentheses. The ab initio/GVFF diagonal force constants for valence angle bending modes are as follows: α13 (O-P-O bending) 0.887/1.510 mdyn Å rad^{-2}; average of α14, α15, α16, α17 (O-P−O bending) 1.250/1.446 mdyn Å rad^{-2}; α18 (O−P−O bending) 1.320/1.490 mdyn Å rad^{-2}; α19, α20 (P−O−C bending) 0.716/0.705 mdyn Å rad^{-2}; average of α21, α22, α23 or α27, α28, α29 (O−C-H bending) 0.683/0.879 mdyn Å rad^{-2}; average of α24, α25, α26 or α30, α31, α32 (H-C-H bending) 0.477/0.572 mdyn Å rad^{-2}. The ab initio/GVFF diagonal force constants for torsional modes are as follows: τ33, τ34 (O−P−O−C torsion) 0.096/0.08 mdyn Å rad^{-2}; τ35, τ36 (P−O−C-H torsion) 0.032/0.038 mdyn Å rad^{-2}.

the two P-O stretching modes (designated P-O/P-O). The ab initio calculation gives 0.195 mdyn Å for this interaction constant. Interaction between the phosphoester stretching modes (P−O/P−O) was calculated to be 0.400 mdyn Å. Similarly, the two interactions between phosphoester and phosphooxy stretching modes (P−O/P-O) are 0.321 and 0.284 mdyn Å.

In previous GVFF calculations on phosphodiesters, it has been assumed that the off-diagonal P-O/P-O term is greater than the P−O/P-O term, which is greater than the P−O/P−O term.[5,36,37,39,40] However, the ab initio calculations indicate that the magnitude of the off-diagonal term is not related directly to bond order. This may reflect the previously mentioned hydration effects, which alter bond orders in the phosphodiester moiety. Additionally, the calculated O−C/C-H interaction (average value 0.163 mdyn Å^{-1}) is not in close agreement with the GVFF value (0.555 mdyn Å^{-1}), and similar discrepancies extend to other off-diagonal force constants of Table 4. A second class of off-diagonal force constants comprises internal coordinates which do not involve a shared atom or bond. Such force constants are expected to be very small and are usually excluded from empirical force fields. However, the present ab initio calculations indicate that not all of the force constants in this class are negligibly small. For example, the P-O/O−C (−0.052 and −0.110 mdyn Å^{-1}) and P−O/C-H (−0.073, −0.052, −0.036 mdyn Å^{-1}) interactions of Table 4 are significant.

It should be recognized that the GVFF force constants constitute only a limited subset of the comprehensive ab initio set, and quantitiative agreement between the two cannot be expected for the off-diagonal terms. Despite these differences in off-diagonal terms, the combined diagonal and off-diagonal force constants of the ab initio force field collectively generate a harmonic force field in substantial agreement with the GVFF results.

3. Vibrational Frequencies and Force Fields for DMP-$^{13}C_2$ and DMP-d_6. Harmonic vibrational frequencies and force fields for the ^{13}C- and ^{2}H-labeled isotopomers, DMP-$^{13}C_2$ and DMP-d_6, were calculated for the optimized structure of Figure 1 using the 3-21+G* basis set. Calculations for DMP-$^{13}C_2$ are compared with experimental results in Table 5. The scaling factors established previously for DMP-h_6 (Table 3) were employed without change for DMP-$^{13}C_2$. This is in accord with normal coordinate analyses indicating that DMP-h_6 and DMP-$^{13}C_2$ are satisfied by the same generalized valence force field.[5] The scaled ab initio frequencies of Table 5 demonstrate good agreement with experimental data, exhibiting an average deviation of 9.84 cm^{-1} (0.89%). Simulated and experimental infrared and Raman spectra are also in good agreement (Figure 4). A clearly discernible effect of ^{13}C substitution is decoupling of C−O and P-O stretching motions, which is manifested for example in the different frequencies and PED values of bands at 1060 and 1051 cm^{-1} due to DMP-h_6 and DMP-$^{13}C_2$, respectively. This result implies that site-specific ^{13}C substitution may be useful generally to decouple vibrational modes of the phosphodiester C−O−P−O−C network in nucleic acids.

Results for DMP-d_6 are given in Table 6 and Figure 5. We noted previously that relatively high anharmonicities in CH stretching and bending modes require appropriate adjustments in force constants for transfer to DMP-d_6.[5] Corresponding adjustments in ab initio scaling factors are indicated in the footnote to Table 6. Other terms in the ab initio force fields of DMP-h_6 and DMP-d_6 are unchanged. The scaled ab initio and experimental frequencies of DMP-d_6 exhibit an average deviation of 12.90 cm^{-1} (1.26%).

Ab initio calculations predict two quasi-degenerate methyl

TABLE 5: Vibrational Frequencies and Potential Energy Distributions for DMP-$^{13}C_2$[a]

ab initio (cm^{-1})					
unscaled	scaled	ab initio PED (%)	Raman (cm^{-1})	NCA PED (%)	assignment
			A Species		
3267	3012	S5(58), S14(42)	3011	S5(100)	ν_a(*CH_3)
3242	2989	S14(50), S5(40), S4(10)	(2987)	S14(100)	ν_a(*CH_3)
3189	2940	S4(89)	2912	S4(100)	ν_s(*CH_3)
1666	1484	S11(90)	1462	S11(82)	δ_a(*CH_3)
1650	1469	S17(92)	1462	S17(82)	δ_a(*CH_3)
1598	1444	S10(97)	1444	S10(93)	δ_s(*CH_3)
1283	1179	S9(77)	1180	S9(68), S11(19), S8(12)	r(*CH_3)
1258	1151	S16(93)	1151	S16(63), S17(18), S12(18)	r(*CH_3)
1164	1082	S1(66), S2(16)	1083	S1(61), S6(16), S2(13)	ν_s(PO_2^-)
1156	1051	S3(56), S1(26), S2(12)	1047	S3(39), S10(30), S2(16), S9(16)	ν_s(*CO)
773	743	S2(55), S3(30)	751	S2(31), S6(17),6(16),S8(16), S9(19), S3(14)	ν_s(PO_2)
551	513	S6(43), S7(36)	501	S6(27), S7(20),S8(20), S13(14)	δ(PO_2^-)
410	387	S15(48), S7(23), S8(11)	390	S15(34), S12(34), S13(32)	τ(PO_2^-)
386	360	S6(44), S7(24), S8(12)	368	S6(35), S7(32), S8(26)	δ(OPO)
228	213	S8(65), S15(28)	(202)	S13(39), S8(36), S15(21)	δ_s(PO*C)
124	124	S13(92)	(141)	S13(92)	τ_s(P−O−*C-H
81	80	S12(88), S7(10)	(71)	S12(92)	τ_s(O−P−O−*C)
			B Species		
3267	3012	S22(59), S27(40)	3011	S22(100)	ν_a(*CH_3)
3241	2989	S27(51), S22(39)	(2987)	S27(100)	ν_a(*CH_3)
3188	2939	S21(90)	2912	S21(100)	ν_s(*CH_3)
1664	1482	S31(90)	1462	S31(82)	δ_a(*CH_3)
1650	1470	S26(90)	1462	S26(82)	δ_a(*CH_3)
1599	1446	S30(95)	1444	S30(100)	δ_s(*CH_3)
1370	1264	S18(95)	1211	S18(37), S28(24), S29(22)	r(*CH_3)
1279	1174	S29(84)	1180	S29(68), S31(19)	r(*CH_3)
1257	1150	S25(94)	1151	S25(65), S26(17), S32(11)	ν_a(PO_2^-)
1136	1034	S20(69), S19(24)	1026	S19(16), S20(38), S30(16)	ν_a(*CO)
815	790	S19(58), S20(22), S23(16)	821	S19(32), S23(29), S24(21)	ν_a(PO_2)
591	559	S28(44), S23(32), S24(17)	538	S28(25), S23(21), S24(18)	r(PO_2^-)
488	463	S23(51), S28(24)	471	S23(46), S28(43)	ω(PO_2^-)
223	208	S24(67), S28(24)	(230)	S24(45), S33(38)	δ_a(PO*C)
143	143	S33(68), S32(22)	(165)	S33(68), S32(26)	τ_a(P−O−*C-H)
105	105	S32(72), S33(27)	(108)	S32(56), S33(41)	τ_a(O−P−O−*C)

av error = 9.84 cm^{-1} (0.89%)

[a] Asterisks indicate the carbon-13 isotope. Other notation is defined in Table 3. Scaling factors are as given in Table 3.

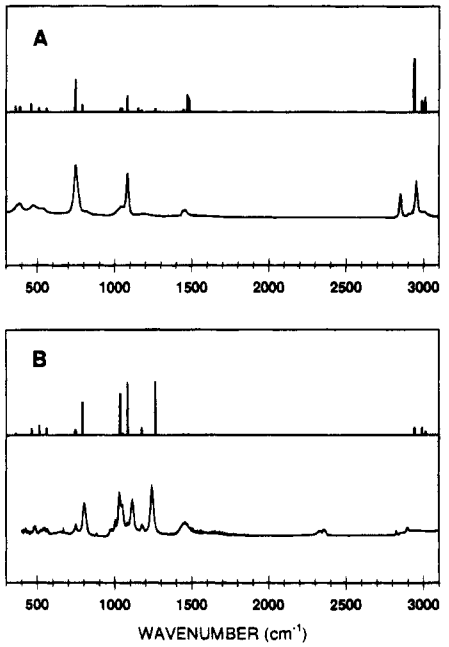

Figure 4. Raman (A) and infrared (B) vibrational spectral of DMP-$^{13}C_2$. In each panel the calculated ab initio frequencies and calculated intensities are represented as bars (upper plot), and the experimental spectrum[5] is shown as a smooth curve (lower plot).

deformation frequencies for DMP-d_6, at 1075 and 1064 cm^{-1}, respectively. Both are lower than the symmetric methyl deformation frequency (1125 cm^{-1}), which represents a reversal of the order observed for DMP-h_6 (Table 3 and ref 5) and other compounds.[40] Table 6 also shows that modes of DMP-d_6 in the 700−1100 cm^{-1} interval are coupled differently than those of DMP-h_6 or DMP-$^{13}C_2$. A similar trend has been identified for isotopomers of diethyl phosphate.[35]

The ab initio results of Tables 3, 5, and 6 indicate that symmetric and antisymmetric P−O stretching modes of DMP-h_6 are lowered only slightly (≈5 cm^{-1}) by ^{13}C substitution, whereas larger depressions (−30 cm^{-1}) result from methyl deuteration. The same phenomenon is observed for diethyl phosphate isotopomers[35] and is consistent with empirical force field calculations.[5] These results suggest that vibrational assignments for bond stretching modes in branched phosphodiester compounds, including nucleic acids, should be approached with extreme caution. Evidently, coupling between skeletal stretching and CH deformation modes cannot be neglected.

Summary and Conclusions

Dimethyl phosphate is the simplest structural analogue of the nucleic acid phosphodiester group. A preference for the *gauche* torsion in phosphoester linkages of DMP enhances its value as a structural model for DNA and RNA, particularly with respect to elucidating vibrational modes diagnostic of the *g,g*-phosphodiester conformation of the nucleic acid backbone. In previous studies, the structure and vibrational spectra of DMP have been investigated using theoretical and experimental approaches.[5,10,11,14,15] The rationale for the present ab initio

TABLE 6: Vibrational Frequencies and Potential Energy Distributions for DMP-d_6[a]

ab initio (cm^{-1})					
unscaled	scaled	ab initio PED (%)	Raman (cm^{-1})	NCA PED (%)	assignment
			A Species		
2433	2269	S5(64), S14(36)	2273	S5(75), S9(14)	$\nu_a(CD_3)$
2411	2249	S14(63), S5(36)	2273	S14(75), S16(14)	$\nu_a(CD_3)$
2286	2133	S4(99)	2088	S4(100)	$\nu_s(CD_3)$
1241	1125	S10(74), S3(13), S1(13)	(1101)	S10(74), S3(16)	$\delta_s(CD_3)$
1177	1106	S2(36), S1(27), S3(27)	1082	S1(36), S11(20), S10(31)	$\nu_s(PO_2^-)$
1211	1075	S11(94)	(1068)	S11(94)	$\delta_a(CD_3)$
1199	1064	S17(94)	(1065)	S17(98)	$\delta_a(CD_3)$
1135	1041	S1(52), S10(24), S3(12)	1056	S3(23), S9(25), S10(25), S2(21)	$\nu_a(CO)$
999	922	S9(76), S3(16)	932	S9(59), S8(20)	$r(CD_3)$
974	903	S16(96)	900	S16(73), S12(17)	$r(CD_3)$
747	715	S2(49), S3(25)	724	S2(24), S3(13), S9(35)	$\nu_s(PO_2)$
540	503	S6(46), S(33)	485	S6(38), S7(26), S8(26)	$\delta(PO_2^-)$
399	377	S15(44), S7(27)	382	S15(53), S7(28)	$\tau(PO_2^-)$
378	353	S6(38), S15(23), S7(21), S8(12)	362	S6(32), S7(28), S8(20)	$\delta(PO_2)$
213	199	S8(71), S15(23)	(188)	S8(40), S13(31)	$\delta_s(POC)$
89	89	S13(94)	(103)	S13(92)	$\tau_s(P-O-C-D)$
73	73	S12(90)	(63)	S12(90)	$\tau_s(O-P-O-C)$
			B Species		
2433	2269	S22(65), S27(34)	2273	S22(75), S29(14)	$\nu_a(CD_3)$
2410	2248	S27(64), S22(34)	2273	S27(75), S24(14)	$\nu_a(CD_3)$
2285	2132	S21(99)	2088	S21(96)	$\nu_s(CD_3)$
1371	1265	S18(95)	1213	S18(44), S28(28)	$\nu_a(PO_2^-)$
1230	1114	S30(94)	1101	S30(78), S3(16)	$\delta_s(CD_3)$
1210	1076	S31(94)	(1068)	S31(95)	$\delta_a(CD_3)$
1197	1064	S26(96)	(1065)	S26(94)	$\delta_a(CD_3)$
1141	1057	S20(48), S19(36)	(1051)	S20(25), S19(25), S29(18)	$\nu_a(CO)$
1005	927	S29(71), S20(16)	932	S29(61), S24(20), S20(17)	$r(CD_3)$
972	901	S25(96)	900	S25(63), S32(17)	$r(CD_3)$
786	757	S19(47), S23(19), S20(17), S29(11)	786	S19(24), S23(28), S29(39)	$\nu_a(PO_2)$
576	545	S28(43), S23(32), S24(14)	527	S28(24), S23(17), S33(14)	$r(PO_2^-)$
481	456	S23(47), S28(26)	465	S23(41), S28(42)	$\omega(PO_2^-)$
206	192	S24(70), S28(22)	(212)	S24(43), S33(28)	$\delta_a(POC)$
123	123	S32(52), S33(39)	(140)	S33(49), S32(34)	$\tau_a(P-O-C-D)$
81	81	S33(59), S32(40)	(85)	S32(59), S33(28)	$\tau_a(O-P-O-C)$

av error = 12.90 cm^{-1} (1.26%)

[a] Notation and scaling factors are as given in Table 3, with the exception of scaling factors of 0.86 for C-D stretching and O-C-D bending.

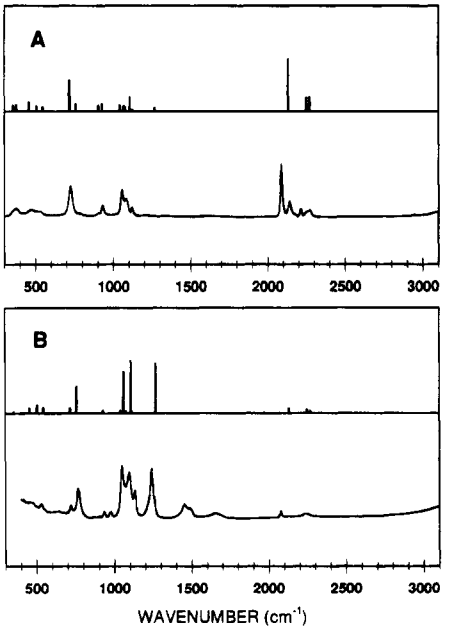

Figure 5. Raman (A) and infrared (B) vibrational spectra of DMP-d_6. In each panel the calculated ab initio frequencies and calculated intensities are represented as bars (upper plot) and the experimental spectrum[5] is shown as a smooth curve (lower plot).

study has been to confirm vibrational assignments based upon normal coordinate analysis and infrared and Raman spectra of DMP isotopomers.[5] We have employed the 3-21+G* basis set at the restricted Hartree–Fock level to obtain a molecular force field and vibrational frequencies of the DMP anion in the optimized *g,g* conformation.

The principal conclusions reached in this study are as follows:

(1) The 3-21+G* ab initio calculations satisfactorily reproduce the infrared and Raman vibrational frequencies, intensities, polarizations and assignments observed for protium, deuterium, and ^{13}C isotopomers of the dimethyl phosphate anion [$(CH_3O)_2PO_2^-$, $(CD_3O)_2PO_2^-$ and $(^{13}CH_3O)_2PO_2^-$]. The consistently good agreement obtained for three isotopic derivatives of DMP implies that ab initio scaling factors employed in the current study should be applicable to other nucleic acid phosphodiester analogues.

(2) The ab initio force field for DMP is consistent with the generalized valence force field (GVFF) determined independently in previous normal coordinate calculations.[5] In particular, the potential energy distributions and diagonal force constants are in excellent agreement for the two sets of calculated normal modes. The empirical force constants appear to be generally reliable, and only a small number of nonbonded off-diagonal force constants is needed to match experimental and calculated (NCA) frequencies.

(3) The ab initio calculations for DMP provide compelling evidence that bond stretching vibrations of phosphodiester linkages and deformation vibrations of methyl substituents are appreciably mixed. This finding suggests that stretching vibrations of 3′ and 5′ phosphoester linkages of nucleic acids are

subject to strong mechanical coupling with deformation modes of the adjoining sugar 3′CH, 4′CH, and 5′CH_2 groups. Accordingly, phosphodiester group vibrational assignments and their conformational significance in DNA and RNA should be interpreted with caution.

(4) The *g,g* conformation of DMP is calculated to be the most stable rotamer and the ab initio optimized structure of the NH_4DMP ion pair is in good agreement with the structure determined by X-ray crystallography. Small structural differences between the DMP anion and NH_4DMP ion pair, which are localized within covalent bonds of the phosphodioxy group, are believed to reflect specific electrostatic interactions in the ion pair.

The present results provide a theoretical foundation for use of the empirical GVFF force field in normal mode analyses of other nucleic acid phosphodiester analogues, including conformational variants. Future studies will focus on ethyl and branched hydrocarbon diesters of the orthophosphate group and on conformations of the C−O−P−O−C network which depart from the *gauche−gauche* configuration considered here.

Acknowledgment. The support of this research by NIH Grant AI18758 (to G.J.T.) is gratefully acknowledged. Support from the American Chemical Society Petroleum Research Fund (to R.G.) is also acknowledged. Y.G. thanks Prof. C. J. Wurrey, Department of Chemistry, University of Missouri−Kansas City, for many hours of helpful discussions and for providing programs to assist in coordinate transformations. Additional programs were made available through the courtesy of Prof. J. R. Durig, Department of Chemistry, University of Missouri−Kansas City.

Supporting Information Available: List of the harmonic force field for the dimethyl phosphate anion (2 pages). Ordering information is given on any current masthead page.

References and Notes

(1) Thomas, G. J., Jr.; Wang, A. H.-J. *Nucleic Acids Mol. Biol.* **1988**, *2*, 1−30.
(2) Thomas, G. J., Jr.; Tsuboi, M. *Adv. Biophys. Chem.* **1993**, *3*, 1−69.
(3) Small, E. W.; Peticolas, W. L. *Biopolymers* **1971**, *10*, 1377−1416.
(4) Thomas, G. J., Jr. *Biochem. Biophys. Res. Commun.* **1971**, *44*, 587−592.
(5) Guan, Y.; Wurrey, C. J.; Thomas, G. J., Jr. *Biophys. J.* **1994**, *66*, 225−235.
(6) Benevides, J. M.; Tsuboi, M.; Wang, A. H.-J.; Thomas, G. J., Jr. *J. Am. Chem. Soc.* **1993**, *115*, 5351−5359.
(7) Thomas, G. J., Jr.; Benevides, J. M.; Overman, S. A.; Ueda, T.; Ushizawa, K.; Saitoh, M.; Tsuboi, M. *Biophys. J.* **1995**, *68*, 1073−1088.
(8) Frisch, M. J.; Head-Gordon, M.; Trucks, G. W.; Foresman, J. B.; Schlegel, H. B.; Raghavachari, K.; Robb, M.; Binkley, J. S.; Gonzalez, C.; Defrees, D. J.; Fox, D. J.; Whiteside, R. A.; Seeger, R.; Melius, C. F.; Baker, J.; Martin, R. L.; Kahn, L. R.; Stewart, J. J. P.; Topiol, S.; Pople, J. A. *Gaussian 90*; Gaussian, Inc., Pittsburgh, PA, 1990.
(9) Fogarasi, G.; Pulay, P. In *Vibrational Spectroscopy and Structure*; Durig, J. R., Ed.; Elsevier: Amsterdam, The Netherlands, 1985, Vol. 14, pp 125−219.
(10) Hadzi, D.; Hodoscek, M.; Grdadolnik, J.; Avbelj, F. *J. Mol. Struct.* **1992**, *266*, 9−19.
(11) Liang, C.; Ewig, C. S.; Stouch, T. R.; Hagler, A. T. *J. Am. Chem. Soc.* **1993**, *115*, 1537−1545.
(12) Curry, B. U. Ph.D. Dissertation, University of California, Berkeley, Univeristy Microfilms International, Ann Arbor, MI.
(13) Berman, H. M.; Olson, W. K.; Beveridge, D. L.; Westbrook, J.; Gelbin, A.; Demeny, T.; Hsieh, S. H.; Srinivasan, A. R.; Schneider, B. *Biophys. J.* **1992**, *63*, 751−759.
(14) Shimanouchi, T.; Tsuboi, M.; Kyogoku, Y. *Adv. Chem. Phys.* **1964**, *7*, 435−498.
(15) Taga, K.; Miyagai, K.; Hirabayashi, N.; Yoshida, T.; Okabayashi, H. *J. Mol. Struct.* **1991**, *245*, 1−11.
(16) Newton, M. D. *J. Am. Chem. Soc.* **1973**, *95*, 256−258.
(17) Gorestein, D. G.; Findlay, J. B.; Momii, R. K.; Luxon, B. A.; Kar, D. *Biopolymers* **1976**, *17*, 3796−3803.
(18) Gorestein, D. G.; Kar, D.; Luxon, B. A.; Momii, R. K. *J. Am. Chem. Soc.* **1976**, *98*, 1668−1673.
(19) Jayaram, B.; Mezei, M.; Beveridge, D. L. *J. Comput. Chem.* **1987**, *8*, 917−942.
(20) Jayaram, B.; Mezei, M.; Beveridge, D. L. *J. Am. Chem. Soc.* **1988**, *110*, 1691−1694.
(21) Giarda, L.; Garbassi, F.; Calcaterra, M. *Acta Crystallogr.* **1973**, *B29*, 1826−1829.
(22) Marynick, D. S.; Schaefer, H. F., III *Proc. Natl. Acad. Sci. U.S.A.* **1975**, *72*, 3794−3798.
(23) Glaser, R.; Streitwieser, A., Jr. *J. Comput. Chem.* **1990**, *11*, 249−264.
(24) Streitwieser, A., Jr.; McDowell, R. S.; Glaser, R. *J. Comput. Chem.* **1987**, *8*, 788−793.
(25) Garrigou-Lagrange, C.; Bouloussa, O.; Clement, C. *Can. J. Spectrosc.* **1976**, *21*, 75−82.
(26) Florian, J.; Baumruk, V. *J. Phys. Chem.* **1992**, *96*, 9283−9287.
(27) Pongor, G.; Pulay, P.; Fogarasi, G.; Boggs. J. E. *J. Am. Chem. Soc.* **1984**, *106*, 2765−2769.
(28) Sutherland, G. B. B. M.; Tsuboi, M. *Proc. R. Soc. London* **1957**, *A239*, 446−463.
(29) Pohle, W.; Bohl, M.; Bohlig, H. *J. Mol. Struct.* **1990**, *242*, 333−342.
(30) Prescott, B.; Steinmetz, W.; Thomas, G. J., Jr. *Biopolymers* **1984**, *23*, 235−256.
(31) Crowe, J. H.; Crowe, L. M.; Chapman, D. *Arch. Biochem. Biophys.* **1984**, *232*, 400−407.
(32) Arrondo, J. L. R.; Goni, F. M.; Macarulla, J. M. *Biochim. Biophys. Acta* **1984**, *794*, 165−168.
(33) Lerner, D. B.; Becktel, W. J.; Everett, R.; Goodman, M.; Kearns, D. R. *Biopolymers* **1984**, *23*, 2157−2172.
(34) Okabayashi, H.; Yoshida, T.; Ikeda, T.; Matsuura, H.; Kitagawa, T. *J. Am. Chem. Soc.* **1982**, *104*, 5399−5402.
(35) Guan, Y.; Thomas, G. J., Jr., to be submitted.
(36) Brown, E. B.; Peticolas, W. L. *Biopolymers* **1975**, *14*, 1259−1271.
(37) Bicknell-Brown, E.; Brown, K. G.; Person, W. B. *J. Raman Spectrosc.* **1982**, *12*, 180−189.
(38) Snyder, R. G.; Zerbi, G. *Spectrochim. Acta* **1967**, *23A*, 391−437.
(39) Wilson, E. B., Jr.; Decius, J. C.; Cross, P. C. *Molecular Vibrations*, McGraw-Hill: New York, 1955.
(40) Durig, J. R.; Nanaie, H.; Guirgis, G. A. *J. Raman Spectrosc.* **1991**, *22*, 155−168.

JP950616O